Geophysical Research Letters

RESEARCH LETTER
10.1029/2022GL098917

# The Role of Boundary Mixing for Diapycnal Oxygen Fluxes in a Stratified Marine System

**P. Holtermann[1], O. Pinner[2], R. Schwefel[3], and L. Umlauf[1]**

[1]Leibniz Institute for Baltic Sea Research, Warnemünde, Germany, [2]Alfred-Wegener-Institute Helmholtz Centre for Polar and Marine Research, Bremerhaven, Germany, [3]Leibniz-Institute of Freshwater Ecology and Inland Fisheries, Berlin, Germany

**Key Points:**

- First direct observation of the seasonality of vertical oxygen fluxes by boundary mixing in one of the largest anoxic systems (Baltic Sea)
- Oxygen fluxes through the halocline are increased by an order of magnitude at the basin boundary
- Boundary mixing contributes more than 80% of the total vertical oxygen transport

**Supporting Information:**

Supporting Information may be found in the online version of this article.

**Correspondence to:**

P. Holtermann,
peter.holtermann@io-warnemuende.de

**Citation:**

Holtermann, P., Pinner, O., Schwefel, R., & Umlauf, L. (2022). The role of boundary mixing for diapycnal oxygen fluxes in a stratified marine system. *Geophysical Research Letters*, *49*, e2022GL098917. https://doi.org/10.1029/2022GL098917

Received 31 MAR 2022
Accepted 4 OCT 2022



**Abstract** Insufficient diapycnal oxygen transport through the halocline is the key reason for the anoxic conditions typically observed in the deeper parts of the Baltic Sea. The variability of turbulent oxygen fluxes through the halocline was investigated seasonally and in space during three cruises (summer, fall, winter). Turbulence dissipation rates and oxygen fluxes showed a pronounced seasonal pattern, with the lowest values during summer. At the basin boundaries, halocline oxygen fluxes increased by an order of magnitude as a result of boundary mixing. A simple box model, distinguishing between interior, intermediate, and boundary regions, was used to extrapolate the locally observed fluxes to the central Baltic Sea. The boundary area, covering less than 23% of the total basin area, contributed more than 80% of the basin-scale oxygen transport through the halocline. According to this model, the annual oxygen flux through the halocline is of the order of 20–28 Gmol per year.

**Plain Language Summary** Oxygen deficits in natural waters are caused by an imbalance of the oxygen demand within a water mass and the transport of oxygen into it. In the Baltic Sea two main water bodies can be distinguished, the surface water and the deep water starting at 80 m. Oxygen is produced by primary production in the upper part while in the deep water the bio-material sink down and require oxygen for their degradation. The strong salinity difference between the deep and the surface water, which is much fresher, creates a transport barrier, that inhibits an oxygen transport from the top to the deeper parts, the halocline. We investigate the seasonal timing and spatial location of the mixing and the transport through the halocline and found the closer the halocline is to the seafloor, the stronger is the mixing and the oxygen flux. There is also a strong seasonality: During the summer months almost no oxygen transport has been observed. In contrast to the fall and winter season with fluxes being at least 10 time larger. With the data available we could quantify the total amount of oxygen being transported through the halocline into the deep parts of the central Baltic Sea.

## 1. Introduction

Over the past decades, the occurrence of suboxic and anoxic zones has significantly increased worldwide with major implications for the affected ecosystems (Conley et al., 2011; Diaz & Rosenberg, 2008, and others). The generation of anoxic water masses in stratified marine systems is related to unbalanced rates of oxygen consumption, production, and transport. Especially in shallow marine and limnic systems, organic matter degradation and in turn oxygen depletion is largely determined by benthic processes and resuspension in the turbulent bottom boundary layer (Glud, 2008). In such systems, turbulent vertical transport of oxygen toward the sediment becomes a key factor in regulating deep-water oxygen dynamics. Lack of sufficient transport mechanisms may lead to permanent anoxia with well-known examples including the Black Sea, the Baltic Sea, and the Cariaco Basin (Astor et al., 2003; Konovalov et al., 2005; Reissmann et al., 2009). For understanding the oxygen dynamics in stratified marine systems, it is thus mandatory to identify and understand the physical transport mechanisms.

Recent research has made considerable progress in identifying and quantifying both oxygen transport processes and oxygen consumption rates. For example, benthic consumption processes, especially relevant in shallow marine systems and lakes, have been studied in various settings using chamber landers, oxygen microprofilers, eddy-covariance techniques, and other approaches (Ahmerkamp et al., 2015; Glud, 2008; Lorke et al., 2003; McGinnis et al., 2014; Noffke et al., 2016, and references therein). Turbulent transport processes in the water column, however, have received much less attention, largely due to the lack of appropriate instrumentation and methodological difficulties related to the strongly intermittent and heterogeneous nature of diapycnal turbulent tracer fluxes. Studies in lakes, coastal seas, and the ocean have shown that vertical mixing is often confined to

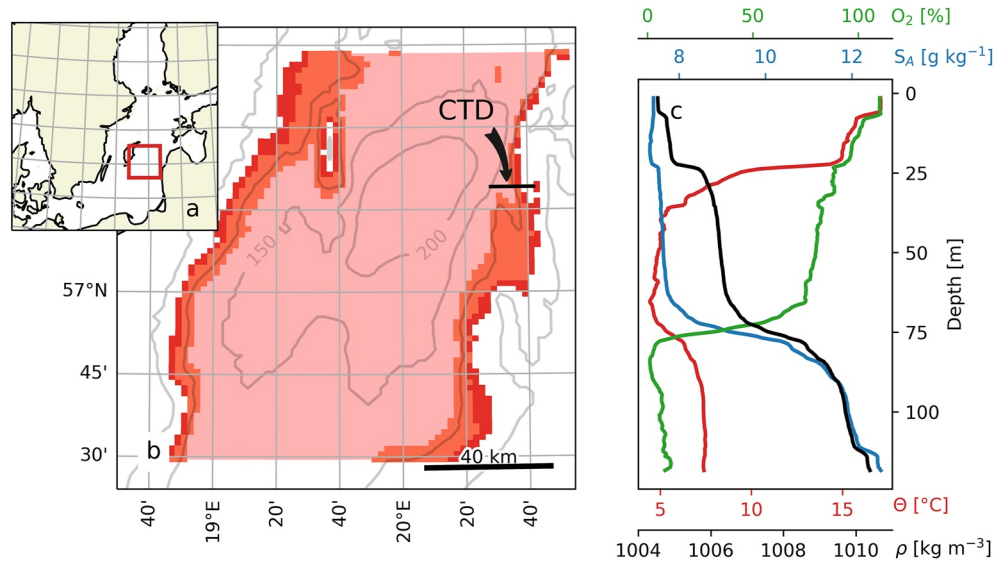


**Figure 1.** Maps of (a) entire Baltic Sea region with study area in the Eastern Gotland Basin marked in red, (b) study area with "boundary," "intermediate," and "interior" regions shaded in red, orange, and pink, respectively. Cross-slope microstructure transect as a black line, arrow indicates the location of the hydrographic profile shown in (c).

the turbulent bottom boundary layers (Ledwell & Hickey, 1995; P. L. Holtermann et al., 2012) and may exhibit a strong seasonal variability (Axell, 1998; P. Holtermann & Umlauf, 2012; Williams et al., 2022). Often both large-scale advective (e.g., Kelly et al., 2020; P. Holtermann et al., 2020) and small-scale turbulent vertical transport (Rovelli et al., 2016) contribute to the total oxygen transport.

Also the lack of suitable sensor technology has restricted the investigation of turbulent oxygen transport processes, in principle fast microelectrodes on microstructure profilers could be used, though their fragility limited the application to a small number of applications for example, Rovelli et al. (2016). The recent establishment of oxygen micro-optodes with response times as small as 0.1 s, combined with easier handling, has opened a promising new approach to directly observe vertical turbulent fluxes, in this study, we will build up on this technique.

Our study is based on high-resolution turbulence and oxygen observations from the central Baltic Sea (Figure 1a), constituting one of the world's largest anoxic marine systems. Tides as the most important energy source for mixing in the ocean are virtually lacking in the Baltic Sea (Reissmann et al., 2009), and the effect of wind-driven near-inertial and topographic waves has been shown insufficient to destabilize the permanent halocline typically located around 60–80 m depth (van der Lee & Umlauf, 2011; P. Holtermann & Umlauf, 2012). This is considered as one of the key reasons for the development of a large volume of sulfidic waters accumulating below the halocline of the central deep basin of the Baltic Sea (P. Holtermann et al., 2020, see also vertical profile in Figure 1b). Except for short periods following so-called Major Baltic Inflows, sporadically occurring on decadal time scales (Gustafsson et al., 2012; P. Holtermann et al., 2014), the basin is in a stagnation period, where the benthic oxygen demand results in gradually increasing $H_2S$ concentrations.

The role of small-scale intrusions, providing an important advective source of oxygen, independent of vertical mixing, has recently been analyzed by P. Holtermann et al. (2020). A surprising result of their study was that the oxygen import through intrusions is largely sufficient to compensate overall oxygen consumption without any indications for a relevant seasonality. This study was, however, based on data from the center of the basin, and could therefore only speculate about the relative importance of boundary mixing. To fill this knowledge gap, here we will investigate the vertical oxygen flux during different seasons across the slope of the central main basin of the Baltic Sea, using a fast-response oxygen sensor in combination with a shear microstructure profiler. The overall goal of this study is to disentangle the relative contributions of oxygen transport and mixing in an anoxic coastal marine system, which will help understanding the generation and future projection of anoxia in the Baltic and other marine systems.

## 2. Sampling and Methods

Turbulence and diapycnal oxygen fluxes were observed along an approximately 12 km long transect on the eastern slope of the Gotland Basin (Figure 1c) during three research cruises with R/V Elisabeth Mann Borgese: EMB169 (fall, 17 October–04 November 2017), EMB177 (winter, 24 February–09 March 2018), and EMB217 (summer, 09–24 July 2019). In total, approximately 1,700 turbulence microstructure profiles were obtained with an MSS90-L microstructure profiler (Sea & Sun technology, Germany), operated in "tow-yo" mode while the ship was slowly moving along the transect, yielding one full-depth profile every 5–8 min, or around 200 m in distance. These cross-slope surveys along the transect were repeated 10–15 times per cruise. Our MSS90 profiler was equipped with two airfoil shear probes for dissipation rate measurements, a fast FP07 thermistor, a Seapoint turbidity sensor, precision CTD sensors, and a fast-response micro-optode (OXR430-UHS-SUB, Pyroscience, Germany) for high-resolution dissolved oxygen measurements. The optode was attached as an external logger (the Turbulent Ocean Data Logger, TODL, developed in-house) to the MSS90 during cruises EMB169 and EMB177, and integrated into the profiler on EMB217. Fast oxygen optodes are known for their drift and require a frequent calibration (Bittig et al., 2018), during each transect oxygen saturations of 0% and 100% air concentration were present and were used for an in situ two point calibration. Dissipation rates (in 0.5 m bins) were calculated from integrating shear spectra across the viscous subrange, correcting for lost variance following the procedure described in Lappe and Umlauf (2016).

Vertical oxygen fluxes were calculated based on a down-gradient expression of the form:

$$F_{O_2} = -\Gamma \frac{\varepsilon}{N^2} \frac{\partial \mathrm{O}_2}{\partial z}, \tag{1}$$

where the turbulent diffusivity $K_\rho$ is expressed in terms of the mixing coefficient $\Gamma$, the turbulence dissipation rate $\varepsilon$, and the (square of the) buoyancy frequency $N^2$ (Osborn, 1980). The oxygen concentration is denoted as $\mathrm{O}_2$, and the $z$-axis is assumed to point vertically upward. The value of the mixing coefficient $\Gamma$ is not unequivocally agreed upon. Here, we use a parameterization suggested by Shih et al. (2005), which predicts a reduction of $\Gamma$ below the canonical value of $\Gamma = 0.2$ for energetic turbulence, quantified via the buoyancy Reynolds number $Re_b = \varepsilon/(\nu N^2)$, where $\nu$ is molecular viscosity. Their model is based on data from homogeneous stratified shear layers, and therefore likely to break down if the distance to the bottom rather than stratification determines the size of the turbulent overturns. We therefore defined a bottom boundary layer based on a density threshold of 0.01 kg m$^{-3}$, inside which we assume that the turbulent diffusivity $K_\rho$ follows the logarithmic wall-layer expression $K_\rho = \varepsilon^{1/3}(\kappa d)^{\frac{4}{3}}$ with the von Kármán constant $\kappa = 0.4$ and the distance to the sea floor $d$. In all cases, we set $F_{O_2} = 0$ if $Re_b < 7$, for which vertical turbulent tracer fluxes have been shown to collapse. It is important to note that in view of the strong intermittency of marine turbulence, applications of Equation 1 require precisely collocated measurements of energy dissipation rates, stratification, and oxygen gradients, based on sensors with fast and comparable response times. The Efron Gong bootstrap resampling method was used for 95% confidence intervals limits of $F_{O_2}$ (Efron & Gong, 1983).

As the halocline shown in Figure 1c constitutes the major obstacle for vertical turbulent transport, the cross-halocline oxygen fluxes are of special interest. The halocline is defined here as the region inside a density interval of ±0.75 kg m$^{-3}$ centered around a density of 1,007 kg m$^{-3}$. This results in average halocline depths and vertical extensions of 70 ± 4 m, 59 ± 2 m and 70 ± 5 m for the cruises EMB169, EMB177, and EMB217, respectively. Figure 2 shows some examples of halocline regions based on this definition. The vertical oxygen flux through the halocline is then defined as the vertical average of the oxygen fluxes across this density interval, computed from Equation 1.

## 3. Results

Transects of oxygen saturation and turbulence dissipation rates, representative for each of the three seasons, respectively, are shown in Figure 2. Stratification and mixing above the halocline show a pronounced seasonal variability: during summer, the seasonal thermocline shelters the deeper halocline layers from surface mixing (Figure 2f), which effectively suppresses halocline erosion by entrainment. During summer and fall, the halocline therefore widens as a result of internal mixing processes (Figures 2b and 2f). Strong wind events in fall finally

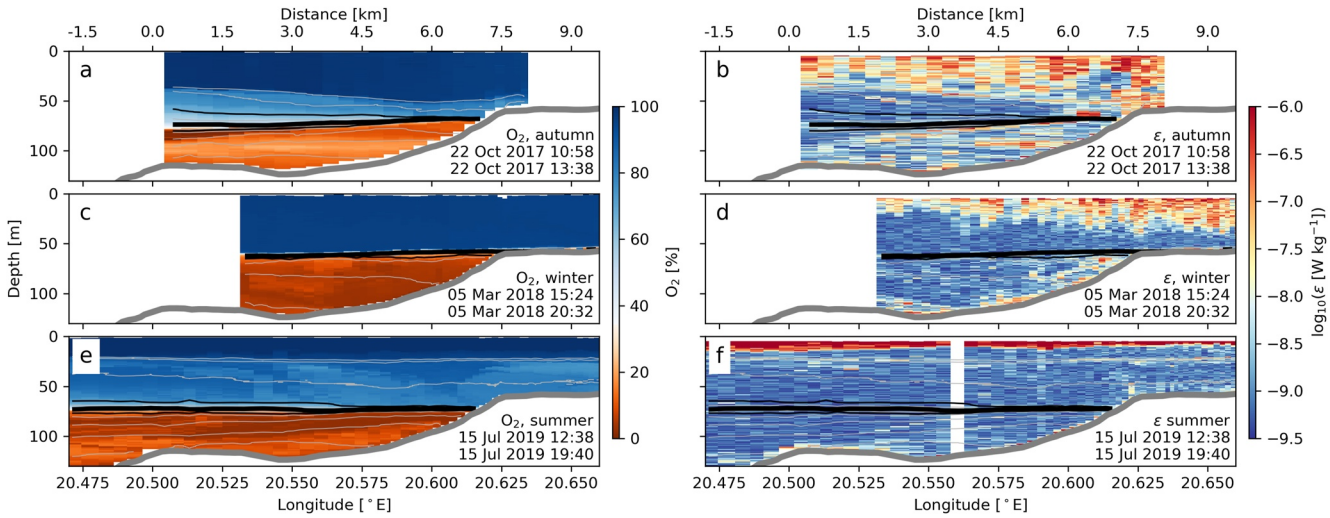


**Figure 2.** Oxygen saturation (left column) and turbulence dissipation rate (right column) along the approximately 12 km long transect shown in Figure 1b for (a, b) fall 2017, (c, d) winter 2018, and (e, f) summer 2019. Thin gray lines indicate isopycnals at 0.5 kg m$^{-3}$ intervals. Isopycnals marking the center of the halocline and its upper and lower edges (see definition in the main text) are shown in black.

erode the seasonal thermocline, however, without fully penetrating down to the halocline (Figure 2b). In winter, surface-layer turbulence is strong enough to initiate erosion of the upper edge of the halocline, generating a sharp density jump at the mixed layer base just above the halocline at 60 m depth (Figure 2d).

Figures 2a, 2c and 2e shows that the vertical distribution of oxygen in the Baltic Sea during all seasons is characterized by an oxic near-surface region and a hypoxic to anoxic deep-water volume below the permanent halocline, emphasizing the crucial effect of this density interface on vertical oxygen transport. Also the seasonal thermocline limits the vertical transport of oxygen in summer and fall, resulting in significantly reduced oxygen concentrations in the intermediate layer between the thermocline and halocline. This highlights the importance of vertical turbulent transport for the local oxygen budget. The variability of oxygen in the region below the halocline, often referred to as the hypoxic transition zone (HTZ, Sommer et al., 2017), is primarily related to the effect of laterally intruding waters with elevated oxygen concentrations, interleaving into the originally anoxic layers (P. Holtermann et al., 2020). Below 150 m depth, this type of intrusions becomes rare, and anoxic conditions are found throughout.

To illustrate the lateral variability of turbulence in the vicinity of the sloping boundary of the basin, we vertically averaged turbulence dissipation rates across the halocline region defined above, and then averaged the resulting cross-slope profiles across all transect surveys performed during the three cruises, respectively, yielding a detailed view of the lateral (i.e., cross-slope) and seasonal variability. As shown in Figure 3, a striking result is the trend of increasing $\varepsilon$ toward the boundary, modulated by a strong seasonality. Lowest dissipation rates were observed during summer with maximum average values around $1 \times 10^{-8}$ W kg$^{-1}$ directly at the boundary, gradually decaying toward $1 \times 10^{-9}$ W kg$^{-1}$ within a distance of approximately 1.5 km. During fall, $\varepsilon$ reaches maximum values up to $5 \times 10^{-7}$ W kg$^{-1}$, again decaying down to a comparable background level over a distance of 3 km. Also in winter, dissipation rates were elevated toward the basin boundary, now, however, with a significant increase up to values around $2 \times 10^{-8}$ W kg$^{-1}$ also in the interior region, away from the boundary.

To investigate how these spatial and seasonal variations in mixing are reflected in the vertical oxygen fluxes, we computed oxygen fluxes across selected isopycnals, spaced at 0.5 kg m$^{-3}$ intervals around the halocline, and, similarly to the dissipation rates, averaged the results over all transect surveys conducted during each of the three cruises, respectively. The diapycnal oxygen fluxes were computed by vertically averaging Equation (1) across vertical density intervals of 0.5 kg m$^{-3}$, centered about each of the selected isopycnals, respectively. Figures 3c–3e shows that, similar to the averaged dissipation rates, also the averaged oxygen fluxes show a striking increase toward the boundary with strongest fluxes observed during the stormy fall season. This forms one of the key results of our study. Note that oxygen fluxes are directed downward only above and inside the halocline. Further, below the halocline, weak upward fluxes can often be discerned in Figures 3c–3e, consistent with the

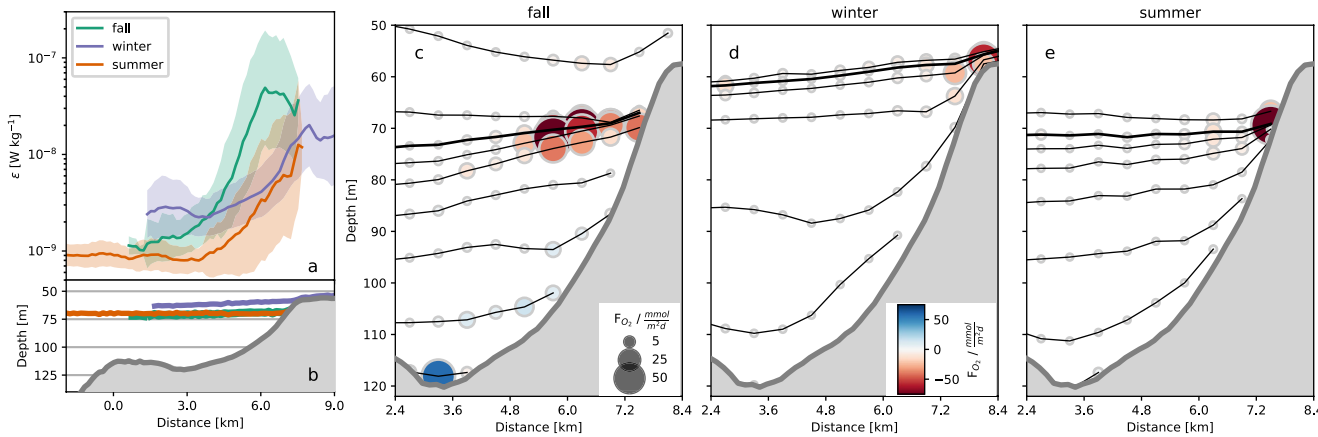


**Figure 3.** Cross-slope variability of (a) cruise-averaged halocline energy dissipation rates, (b) bathymetry (in gray) and average halocline depths for the three cruises, respectively, and (c–e) cruise-averaged downward oxygen fluxes for fall, winter, and summer, respectively. Shaded areas in (a) mark one standard deviation of the natural variability encountered on the individual transect surveys. Circle markers in (c–e) indicate diapycnal oxygen fluxes across selected isopycnals (black) spaced at 0.5 kg m$^{-3}$ intervals in the vicinity of the halocline. The size of the symbols indicates the magnitude of the fluxes, the color (red = downward, blue = upward) their direction as shown in the legends. Thick black isopycnals mark the halocline. Gray-shaded areas indicate the bathymetry.

slightly negative (average) oxygen gradient in this upper part of the HTZ (e.g., Figure 1c). This peculiar structure of the oxygen profiles can be explained by the effect of oxic intrusions into the HTZ as discussed in detail in P. Holtermann et al. (2020).

Mixing in the central Baltic Sea is mainly wind driven and correlates with the wind speed cubed, $|\mathbf{U}_w|^3$ (Axell, 1998), with single wind events triggering wave motions decaying on time scales of weeks (P. Holtermann & Umlauf, 2012). We use this to investigate to what degree the derived oxygen fluxes are representative for their respective seasons. This was done by comparing the wind situation in the time period of each cruise including 7 days before the first sampling with the long-term Coastdat2 re-analysis data (Groll & Weisse, 2017) between 1948 and 2020. While $|\mathbf{U}_w|^3$ of the autumn cruise is well within the long term average, the summer/winter cruises show a significantly increased/decreased $|\mathbf{U}_w|^3$, Table 1 first column.

**Table 1**
*Left: Wind Speed Cubed in 10 m Height at 57.35°N, 20.08°E Between 1948 and 2020 and During the Research Cruises*

| | $\lvert\mathbf{U}_w\rvert^3$ | | $F_{O_2}$ transect | | | $M_{O_2}$ basin | | |
|---|---|---|---|---|---|---|---|---|
| | 1948–2020 | Cruise | Boundary | Intermed | Interior | Boundary | Intermed | Interior |
| Season | [m$^{-3}$ s$^{-3}$] | | [mmol m$^{-2}$ d$^{-1}$] | | | [Gmol y$^{-1}$] | | |
| Spring | 586 | – | – | – | – | – | – | – |
| | ±127 | – | – | – | – | – | – | – |
| Summer | 430 | 542 | **−16** (47%) | **−4** (57%) | **−0.3** (60%) | **−5** | **−4** | **−1** |
| | ±72 | | −39 to −2 | −7 to −2 | −0.4 to −0.2 | −13 to −1 | −5 to −2 | −2 to −1 |
| Fall | 1012 | 1039 | **−19** (38%) | **−37** (8%) | **−1.2** (11%) | **−6** | **−30** | **−4** |
| | ±181 | | −34 to −6 | −48 to −27 | −2.2 to −0.4 | −11 to −2 | −39 to −22 | −8 to −1 |
| Winter | 1224 | 906 | **−14** (36%) | **−4** (35%) | **−1.9** (65%) | **−5** | **−4** | **−8** |
| | ±285 | | −19 to −9 | −6 to −3 | −2.7 to −1.2 | −7 to −3 | −5 to −3 | −11 to −5 |
| Year low | | | **−17** | **−21** | **−1.1** | **−6** | **−17** | **−4** |
| (spring = summer) | | | −31 to −6 | −27 to −15 | −1.9 to −0.5 | −10 to −2 | −22 to −12 | −7 to −2 |
| Year high | | | **−16** | **−12** | **−0.9** | **−5** | **−10** | **−4** |
| (spring = fall) | | | −33 to −5 | −17 to −9 | −1.4 to −0.5 | −11 to −2 | −14 to −7 | −6 to −2 |

*Note*. In Bold regional and seasonal contributions of halocline oxygen fluxes observed along the transect (center) and yearly oxygen flux extrapolated to the entire basin (right). In brackets percentage of samples with $Re_b < 7$ (collapsing turbulent fluxes), second line 95% percentile confidence intervals.

## 4. Discussion and Conclusions

To systematically quantify the contribution of boundary mixing to the overall basin-scale diapycnal oxygen fluxes, it is helpful to distinguish between different regions according to their proximity to the lateral slopes of the basin. For this purpose, we use the distance $D_{hs}$ between the halocline and the sediment to define three distinct regions: a "boundary" region with $D_{hs} < 10$ m, where halocline mixing is directly fueled by bottom-generated turbulence; an "interior" region with $D_{hs} > 40$ m, where weak oxygen fluxes are driven by sporadic local shear-instabilities (e.g., Lappe & Umlauf, 2016); and finally an "intermediate" region ($10 < D_{hs} < 40$ m) that is only partly affected by boundary mixing processes. A more detailed discussion of the rationale behind this choice is provided in Supporting Information S1.

For each profile taken along our transect, we calculated the oxygen fluxes across the halocline and sorted them into one of these three subregions. The region-averaged fluxes for each season as well as the annual average are summarized in Table 1. For the computation of the annual average, we assumed that the oxygen fluxes in spring (where no data were collected) correspond to those of either fall or summer, representing the periods with strongest and weakest turbulent fluxes, respectively.

The resulting annual mean for the case spring = summer can thus be thought of as a lower limit, since the winter cruise showed a decreased $|\mathbf{U}_w|^3$ and the averaged spring $|\mathbf{U}_w|^3$ is larger compared to the summer cruise. Based on this it is fair to assume that both winter and spring fluxes are typically higher. The low wind speeds during the winter cruise make the upper limit much less certain. It is clear that an increased wind will also increase the vertical oxygen flux but the interplay between the very strong stratification omit a valid prediction and points to the need of further research of turbulent mixing processes during the winter months.

Histograms of the regionally sorted fluxes (not shown) reveal that during all seasons, a large fraction of the samples is characterized by vanishing fluxes due to buoyancy Reynolds numbers below the threshold for collapsing turbulence (Table 1), suggesting that the turbulent fluxes are strongly intermittent. To compute stable averages, a large number of transect surveys (10–15 in this case) with densely-spaced microstructure profiling was thus required during each of the three cruises.

The most obvious conclusion from Table 1 is that the annual oxygen fluxes in the "interior" region are at least an order of magnitude smaller compared to both the "boundary" and "intermediate" regions, highlighting the importance of boundary mixing. The stormy fall season dominates the annual fluxes in the "intermediate" region, yearly averaged fluxes for the "boundary" and "intermediate" regions are on the order of 10 mmol $m^{-2}$ $d^{-1}$, that is, comparable to typical values for the benthic oxygen demand (Sommer et al., 2017). This suggests that turbulent oxygen fluxes through the halocline may be, at least locally, a relevant factor. We will come back to this point below.

Assuming that the average halocline depth (66 m) of the three cruises is representative for the entire basin, the subregions defined above can be extrapolated to the entire basin. For consistency with the oxygen budget constructed in P. Holtermann et al. (2020), we define the northern and southern boundaries of our domain identical to their "central" region, leading to the subregions shown in Figure 1. From this analysis, it can be shown that 77% of the entire basin area are covered by the "interior" region, followed by the "intermediate" and "boundary" regions with contributions of 17% and 6%.

Similarly, also the observed oxygen fluxes through the halocline can be extrapolated to the entire basin. The key underlying assumption for this is, obviously, that boundary mixing processes are comparable everywhere along the lateral slopes of the basin. We lack an independent verification of this assumption; some support, however, is provided by P. Holtermann and Umlauf (2012), who showed that boundary mixing processes are driven by different types of basin-scale motions (topographic and near-inertial waves) that are likely affecting all slope regions in similar ways. Multiplying the fluxes found in the different subregions with their respective basin-wide areas results in the basin-averaged oxygen fluxes compiled in Table 1. Outstanding are the contributions of the "boundary" and "intermediate" regions, which, despite their small areas, taken together account to more than 80% of the total turbulent oxygen flux of 20–28 Gmol (with a bootstrapping confidence interval of 11–39 Gmol) per year through the halocline.

Based on these estimates and earlier studies, we attempt to summarize the present knowledge on oxygen transport and transformation pathways in Figure 4. There, our pelagic oxygen flux estimates are compared to the

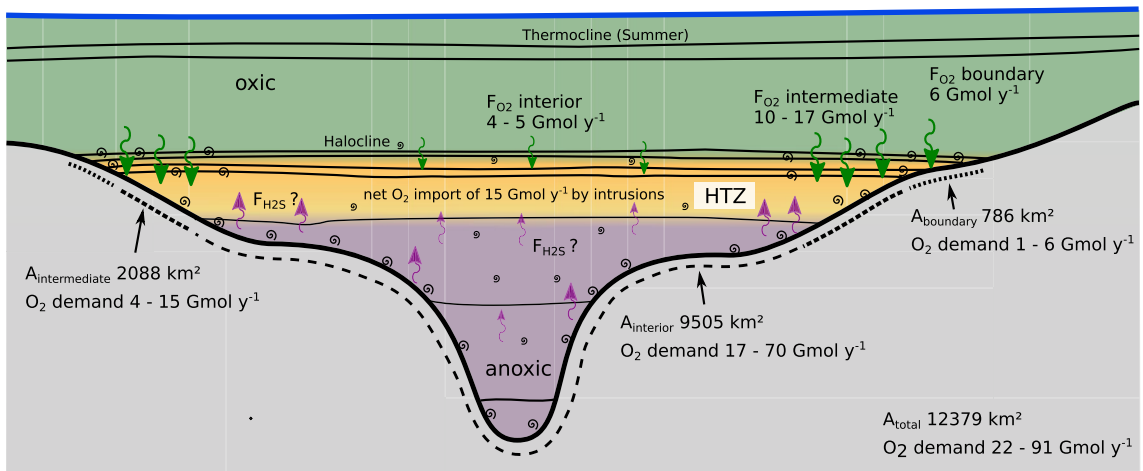


**Figure 4.** Oxygen transport and transformation pathways in the central Baltic Sea. Black lines indicate isopycnals. Whirls mark turbulent regions and arrows show oxygen and $H_2S$ transport pathways.

benthic oxygen demand, for which values in the range 5–20 mmol $m^{-2}$ $d^{-1}$ have been reported for oxic sediments (Noffke et al., 2016; P. Holtermann et al., 2020). For anoxic sediments in the deeper part of the basin, Sommer et al. (2017) suggest $H_2S$ fluxes in the range 3–10 mmol $m^{-2}$ $d^{-1}$ at the sediment-water interface, which, based on the stoichiometry for the oxidation of sulfide to sulfate, requires an oxygen flux of 6–20 mmol $m^{-2}$ $d^{-1}$. From a budget point of view, therefore, the oxygen demand of the anoxic and oxic parts of the basin is comparable. Despite the relatively large uncertainty in the estimated oxygen demand, a strong oxygen deficit in the "interior" region becomes evident, induced by the oxygen required to re-oxidize $H_2S$ (and likely also other reduced substances) diffusing upward from the sediment-water interface.

Assuming that turbulent oxygen fluxes are negligible and that the benthic oxygen demand is the main oxygen sink in the HTZ, P. Holtermann et al. (2020) showed that an amount of approximately 30 Gmol per year is imported into the HTZ by lateral intrusions. As approximately half of the oxygen imported by the intrusions leaves the HTZ again (P. Holtermann et al., 2020), the net import is approximately 15 Gmol. Our direct turbulent flux measurements, however, show that their assumption of negligible turbulent oxygen transport only holds during the summer period when the wind forcing is weak. In view of the 4–5 Gmol mixed across the halocline in the interior region per year (Figure 4), the net amount of oxygen imported by intrusions therefore has to be corrected downward to approximately 10 Gmol.

The most plausible picture is thus the following (Figure 4): During the summer months, when mixing is negligible, the total oxygen demand inside the HTZ (mostly benthic) is compensated by lateral intrusions. During times with strong wind forcing, turbulent oxygen fluxes through the halocline become a relevant factor especially near the boundaries. A part of this oxygen is directly supplied to the sediment at locations where the halocline intersects with the sloping topography. A larger fraction is used to reoxidize reduced substances like $H_2S$ at the lower edge of the HTZ, since their fluxes will increase during fall/winter, we suggest that the overall reoxidation process will be intensified. It is unlikely that local vertical mixing and local oxygen demand perfectly balance, suggesting additional lateral transport pathways, including the intrusions mentioned above, to communicate dissolved substances between the interior region and the transformation hot spots near the slopes.

In the light of understanding the consequences of the changing climate with its impact on wind forcing and stratification (Hordoir et al., 2018; Stigebrandt & Gustafsson, 2003), it is of importance to further study the specific processes causing the oxygen transport. The wide-spread relevance of boundary mixing also in other anoxic marine and limnic systems makes it likely that similar mixing and transport processes are relevant also beyond the Baltic Sea.

## Data Availability Statement

All data and source code for the processing is available under the DOI: https://doi.org/10.12754/data-2022-0002.

**Acknowledgments**
We like to thank the captain and crew of R/V Elisabeth Mann Borgese for their flexibility and reliable professional support during the three cruises presented in this article. Excellent technical support by Martin Sass and Toralf Heene is greatly appreciated. P. Holtermann is thankful for the support by the German Research Foundation (DFG) through Grant HO 5891/1-1. Robert Schwefel was funded by Swiss National Science Foundation (Grant 178230). Open Access funding enabled and organized by Projekt DEAL.

## References

Ahmerkamp, S., Winter, C., Janssen, F., Kuypers, M. M. M., & Holtappels, M. (2015). The impact of bedform migration on benthic oxygen fluxes. *Journal of Geophysical Research: Biogeosciences*, *120*(11), 2229–2242. https://doi.org/10.1002/2015JG003106

Astor, Y., Muller-Karger, F., & Scranton, M. I. (2003). Seasonal and interannual variation in the hydrography of the Cariaco Basin: Implications for basin ventilation. *Continental Shelf Research*, *23*(1), 125–144. https://doi.org/10.1016/S0278-4343(02)00130-9

Axell, L. B. (1998). On the variability of Baltic Sea deepwater mixing. *Journal of Geophysical Research*, *103*(C10), 21667–21682. https://doi.org/10.1029/98JC01714

Bittig, H. C., Körtzinger, A., Neill, C., van Ooijen, E., Plant, J. N., Hahn, J., et al. (2018). Oxygen optode sensors: Principle, characterization, calibration, and application in the ocean. *Frontiers in Marine Science*, *4*. https://doi.org/10.3389/fmars.2017.00429

Conley, D. J., Carstensen, J., Aigars, J., Axe, P., Bonsdorff, E., Eremina, T., et al. (2011). Hypoxia is increasing in the coastal zone of the Baltic Sea. *Environmental Science & Technology*, *45*(16), 6777–6783. https://doi.org/10.1021/es201212r

Diaz, R. J., & Rosenberg, R. (2008). Spreading dead zones and consequences for marine ecosystems. *Science*, *321*(5891), 926–929. https://doi.org/10.1126/science.1156401

Efron, B., & Gong, G. (1983). A leisurely look at the bootstrap, the jackknife, and cross-validation. *The American Statistician*, *37*(1), 36–48. https://doi.org/10.1080/00031305.1983.10483087

Glud, R. N. (2008). Oxygen dynamics of marine sediments. *Marine Biology Research*, *4*(4), 243–289. https://doi.org/10.1080/17451000801888726

Groll, N., & Weisse, R. (2017). A multi-decadal wind-wave hindcast for the north sea 1949–2014: CoastDat2. *Earth System Science Data*, *9*(2), 955–968. https://doi.org/10.5194/essd-9-955-2017

Gustafsson, B. G., Schenk, F., Blenckner, T., Eilola, K., Meier, H. E. M., Müller-Karulis, B., et al. (2012). Reconstructing the development of Baltic Sea eutrophication 1850–2006. *Ambio*, *41*(6), 534–548. https://doi.org/10.1007/s13280-012-0318-x

Holtermann, P., Burchard, H., Gräwe, U., Klingbeil, K., & Umlauf, L. (2014). Deep-water dynamics and boundary mixing in a non-tidal stratified basin. A modeling study of Baltic Sea. *Journal of Geophysical Research*, *119*(2), 1465–1487. https://doi.org/10.1002/2013JC009483

Holtermann, P., Prien, R., Naumann, M., & Umlauf, L. (2020). Interleaving of oxygenized intrusions into the Baltic Sea redoxcline. *Limnology & Oceanography*, *65*(3), 482–503. https://doi.org/10.1002/lno.11317

Holtermann, P., & Umlauf, L. (2012). The Baltic Sea tracer release experiment. 2. Mixing processes. *Journal of Geophysical Research*, *117*(C1), C01022. https://doi.org/10.1029/2011JC007445

Holtermann, P. L., Umlauf, L., Tanhua, T., Schmale, O., Rehder, G., & Waniek, J. J. (2012). The Baltic Sea tracer release experiment: 1. Mixing rates. *Journal of Geophysical Research*, *117*(C1), C01021. https://doi.org/10.1029/2011JC007439

Hordoir, R., Höglund, A., Pemberton, P., & Schimanke, S. (2018). Sensitivity of the overturning circulation of the Baltic Sea to climate change, a numerical experiment. *Climate Dynamics*, *50*(3), 1425–1437. https://doi.org/10.1007/s00382-017-3695-9

Kelly, S., de Eyto, E., Dillane, M., Poole, R., & White, M. (2020). Characterizing ventilation events in an anoxic coastal basin: Observed dynamics and the role of climatic drivers. *Limnology & Oceanography*, *65*(10), 2420–2442. https://doi.org/10.1002/lno.11462

Konovalov, S. K., Murray, J. W., & Luther, G. I. W. (2005). Black Sea biogeochemistry. *Oceanography*, *18*(2), 24–35. https://doi.org/10.5670/oceanog.2005.39

Lappe, C., & Umlauf, L. (2016). Efficient boundary mixing due to near-inertial waves in a nontidal basin: Observations from the Baltic Sea. *Journal of Geophysical Research: Oceans*, *121*(11), 8287–8304. https://doi.org/10.1002/2016JC011985

Ledwell, J. R., & Hickey, B. M. (1995). Evidence for enhanced boundary mixing in the Santa Monica basin. *Journal of Geophysical Research*, *100*(C10), 20665–20679. https://doi.org/10.1029/94JC01182

Lorke, A., Müller, B., Maerki, M., & Wüest, A. (2003). Breathing sediments: The control of diffusive transport across the sediment—Water interface by periodic boundary-layer turbulence. *Limnology & Oceanography*, *48*(6), 2077–2085. https://doi.org/10.4319/lo.2003.48.6.2077

McGinnis, D. F., Sommer, S., Lorke, A., Glud, R. N., & Linke, P. (2014). Quantifying tidally driven benthic oxygen exchange across permeable sediments: An aquatic eddy correlation study. *Journal of Geophysical Research: Oceans*, *119*(10), 6918–6932. https://doi.org/10.1002/2014JC010303

Noffke, A., Sommer, S., Dale, A. W., Hall, P. O. J., & Pfannkuche, O. (2016). Benthic nutrient fluxes in the Eastern Gotland Basin (Baltic Sea) with particular focus on microbial mat ecosystems. *Journal of Marine Systems*, *158*, 1–12. https://doi.org/10.1016/j.jmarsys.2016.01.007

Osborn, T. R. (1980). Estimates of the local rate of vertical diffusion from dissipation measurements. *Journal of Physical Oceanography*, *10*(1), 83–89. https://doi.org/10.1175/1520-0485(1980)010<0083:eotlro>2.0.co;2

Reissmann, J., Burchard, H., Feistel, R., Hagen, E., Lass, H.-U., Mohrholz, V., et al. (2009). Vertical mixing in the Baltic Sea and consequences for eutrophication – a review. *Progress in Oceanography*, *82*(1), 47–80. https://doi.org/10.1016/j.pocean.2007.10.004

Rovelli, L., Dengler, M., Schmidt, M., Sommer, S., Linke, P., & McGinnis, D. F. (2016). Thermocline mixing and vertical oxygen fluxes in the stratified central North Sea. *Biogeosciences*, *13*(5), 1609–1620. https://doi.org/10.5194/bg-13-1609-2016

Shih, L. H., Koseff, J. R., Ivey, G. N., & Ferziger, J. H. (2005). Parameterization of turbulent fluxes and scales using homogeneous sheared stably stratified turbulence simulations. *Journal of Fluid Mechanics*, *525*, 193–214. https://doi.org/10.1017/S0022112004002587

Sommer, S., Clemens, D., Yücel, M., Pfannkuche, O., Hall, P. O. J., Almroth-Rosell, E., et al. (2017). Major bottom water ventilation events do not significantly reduce basin-wide benthic N and P release in the eastern Gotland Basin (Baltic Sea). *Frontiers in Marine Science*, *4*. https://doi.org/10.3389/fmars.2017.00018

Stigebrandt, A., & Gustafsson, B. G. (2003). Response of the Baltic Sea to climate change—Theory and observations. *Journal of Sea Research*, *49*(4), 243–256. https://doi.org/10.1016/S1385-1101(03)00021-2

van der Lee, E. M., & Umlauf, L. (2011). Internal wave mixing in the Baltic Sea: Near-inertial waves in the absence of tides. *Journal of Geophysical Research*, *116*(C10), C10016. https://doi.org/10.1029/2011JC007072

Williams, C. a. J., Davis, C. E., Palmer, M. R., Sharples, J., & Mahaffey, C. (2022). The three Rs: Resolving respiration robotically in Shelf Seas. *Geophysical Research Letters*, *49*(4), e2021GL096921. https://doi.org/10.1029/2021GL096921